Algerian Journal of Environmental Science and Technology
March edition. Vol.9. N°1. (2023)
ISSN : 2437-1114
www.aljest.org

Investigation of microgalvanic activity of carbon steel API 5L X52 in presence of Amine corrosion inhibitors by scanning vibrating electrode technique (SVET)

I.Ouarzki[1*], M. Bounoughaz[1,2*]

[1]Laboratory of bioinformatics, applied microbiology, and biomolecules (BMAB), Faculty of sciences, University of M'hamed Bougara, Boumerdes,35000, Algeria
[1,2]Laboratory of treatment and forming of polymers, Faculty of Technology, University of M'hamed Bougara, Boumerdes, 35000, Algeria

*Corresponding author: ouarzkimane@yahoo.fr, moussa_bounoughaz@yahoo.fr

ARTICLE INFO

Article History :

Received ***: 14/01/2020***
Accepted ***: 25/05/2021***

***Key Words*:**
Corrosion*; SVET ; microgalvanic activity; corrosion inhibitors.*

ABSTRACT/RESUME

Abstract: *Microgalvanic activity of carbon steel API 5L X52 was investigated by scanning vibrating electrode technique (SVET). Two types of corrosion inhibitors were used for the protection of carbon steel. The first one is based on primary amine function with linear carbon chain (inhibitor A).The second one contains primary amine with Ethylene oxide branched chain (inhibitor B). The evolution of microgalvanic activity was studied at different imposed currents ranging up to 200 mA without and in the presence of 20 ppm and 50 ppm of each corrosion inhibitor. In absence of inhibitors, the maps given by SVET analysis showed a uniform microgalvanic activity with imposed currents ranging from 0 to 1 mA and tend towards less cathodic area. For high imposed currents (10mA, 25mA, 50mA, 100mA and 200mA); a clear evolution in the microgalvanic activity is noticed considering the presence of several anodic area. The dissolution of the carbon steel was accelerated and the microgalvanic potential tends to electronegative values. With the corrosion inhibitors, no anodic area was observed for weak currents ranging from 0 to 10mA. The best protection is assured by the inhibitor B due to the improvement of its solubility. Beyond 25 mA, the protection from corrosion decreases but inhibitor B still demonstrates a better efficiency.*

I. Introduction

The corrosion mechanisms and electrochemical behavior of carbon steel have been investigated in several works, pitting corrosion [1-3], crevice corrosion [4-6], bacterial corrosion [7-9] and galvanic corrosion [10-12]. Microgalvanic corrosion has been always a serious problem in the industry especially in oil industry. This is due to the many pipelines and equipment damages resulting from the heterogeneous process occurring on corroding metal surface exposed to an aggressive environment [13].

To deal with corrosion problems, several methods were used to characterize corrosion behavior such as electrochemical techniques [14-18] which are considered as a sensitive method [14]. Unlike other methods, SVET gives information about the type, morphology of corrosion attack and the nature of microgalvanic activity. This technique has been used since 1980. It allows to investigate many materials and it finds application in the studies of corrosion process [19, 20]. [21] have studied the galvanic corrosion of the iron/zinc system in 0.1 M Na_2SO_4 aqueous solution at ambient temperature. SVET results provide an excellent spatial

resolution and let observe zinc oxidation started in localized regions.
Regarding [22], SVET results indicate the microgalvanic activity evolution ant it explore the efficiency of corrosion inhibitors under different imposed currents. Organic compounds with NH_2, -COOH, -OH functions are the most efficient corrosion inhibitors [23] because they form an adsorbed protecting barrier on the metal surface. Inorganic compounds such as chromate, dichromate and nitrites proved good performance as corrosion inhibitors for the carbon steel but its application is limited because of their toxicity for the environment [24]. The evaluation of the efficiency of corrosion inhibitors using SVET in aqueous environment [25] has been approached for different materials. The API 5L X52 carbon steel is widely used in oil and gas industries. Because of the corrosive medium related to the oil and gas production [26]; many additives have been proposed such as corrosion inhibitors which are the most convenient way for metal protection. These compounds are alkyl or aryl amines [27]. Several types of corrosion inhibitors are currently used in the process of natural gas and oil refining. It's reported also that amine function is used in the formulation of corrosion inhibitors and shows a good efficiency for the protection of carbon steel [28-32]. However SVET gave information about corrosion rate and morphology but could not detect nucleation and passivation phenomena on the surface of carbon steel electrodes [31].

In the present work SVET technique is used to compare two types of commercial inhibitors containing primary amine with linear carbon chain (Inhibitor A) and Ethylene oxide branched chain (inhibitor B) for the protection of the carbon steel. A series of experiments were conducted in aqueous environment to display and locate electrochemical phenomena on the working electrode. Anodic currents were applied in the absence and in the presence of corrosion inhibitors to evaluate their effects on the sweeping surface. The evolution in the electrode potential is represented by maps of the micro galvanic activities that allow the identification of the electrochemical behavior of the surface, and the effect of the addition of the corrosion inhibitors on the electrochemical behavior that can take place as function of the time.

II. Materials and methods

II.1 Experimental setup

SVET SVP100 is used to study the microgalvanic activity of API5LX52 carbon steel in aqueous environment (NaCl 35g/l). It is composed by electronic unit of the probe of computer and Potentiostat-Galvanostat. The probe is immersed in 5 litter cell and driven by a motor that provides a three-dimensional displacement X (as abscissa), Y (ordinate) and Z (in space). The SVP100 system demonstrates in real-time the local electrochemical activity on the carbon steel. The scheme of the equipment is showed in Figure.1.

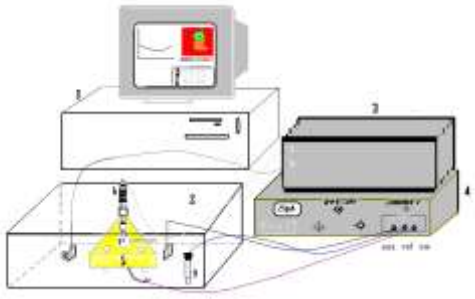

Figure 1. *Representative scheme of SVET*

1) Central unit
2) Electrolytic tank
3) Main scanning unit (SVP100)
4) Potentiostat-Galvanostat
5) Sample holder (tripod)
6) Platinum probe (vibratory reference electrode)
7) Sample to be analyzed
8) Counter electrodes (auxiliary electrodes)
9) Reference electrode (with saturated calomel)

II.2. Experimental conditions

The electrolytic medium is formed by distilled water and 35 g/l of NaCl (ASTM medium). This medium was acidified with HCl (pH ≈ 3, conductivity ≈ 1300 S cm−1) to make it acidic solution and to let corrosion proceed and produce ohmic drops, which can be measured by SVET [32]

II.3. Scanning vibrating electrode technique (SVET)

The SVET employed in this work was a commercial Perkin Elmer SVP100 (Uniscan). The basic parameters employed during the tests are listed in Table 1. For each test, SVET cell was filled with 800 mL of working solution. The tests were repeated twice to check the repeatability of the results. In order to acquire proper SVET data, a typical calibration procedure must be carried out. The parameters defined during calibration are only valuable for the same probe-solution pair. Making the assumption that the electric field is constant around the probe's course, the calibration was performed employing a gold point in space (PIS) electrode connected to a galvanostat immersed in the working solution and placed 150 µm above

PIS's surface. The probe was made to vibrate (50 µm peak-to-peak). Then, by applying a current of 2 A, the sensitivity was adjusted to keep the output signal between 10% and 70% and to obtain the optimal phase. Subsequently, the imposed current was varied (between +8 A and −8 A) to verify that the signal did not saturate. Experimental conditions are summarized in tables 1 and 2.
The displacement of the probe towards the scanned area is given following the execution of the menu probe control as shown in table2.

Table 1. *Experimental conditions of the SVET experiments*

Temperature	Ambiant (25°C)
Pressure	Atmospheric
Electrolyte	NaCl, 35g/l
PH	3

Table 2. *SVET operational conditions during the experiments.*

Scanning mode	surface
Number of lines	512
Displacement following abscissa X	18000
Displacement following the ordinate Y	¾ of X
Scanning speed	1000
Sensitivity	10 µV
Reference phase	60
Amplitude	10
Volume of solution	800ml

Inhibitors A and B are film-forming cathodic inhibitors extensively employed in the protection of a variety of metals [23, 24, 26–29]. The inhibitor A is a commercial corrosion inhibitor supplied by CHIMEC company. The product A is a balanced mixture of compounds with a different volatility providing an appropriate film on all metal surfaces.
It is recommended as corrosion inhibitor for equipment of oil and gas production in oil field. It is stated to contain a blend of aliphatic amines and amine derivatives in a high boiling point solvent (1, 2, 4 trimethylbenzene). It is a brown liquid and is completely soluble in hydrocarbons and dispersible in water. The inhibitor B is a commercial corrosion inhibitor supplied by CHIMEC company. The product B is recommended as corrosion inhibitor for oil, gas and water facilities. It is stated to contain (MSDS) amide/imidazolines (10.0-30.0 %), quaternary ammonium salts (5.0-10.0 %), propan-2-ol (10.0-30.0 %), methanol (1.0-5.0 %), and acetic acid (1.0-5.0 %). It is a liquid with a characteristic odour and it is soluble in water.
The experiments were carried out in the same operating conditions under electric currents up to 200 mA in presence and absence of corrosion inhibitors A and B. The concentration of 20 ppm and 50 ppm has been chosen as used in the oil industry. The aim of this work was to see the effect of the anode currents applied on the performance of the two inhibitors. The results given by SVET are represented by following maps

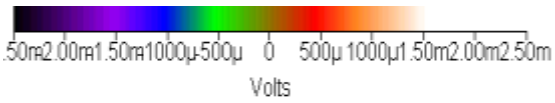

According to the American convention, cathodic domains are represented by the light colors, preceded by a sign (+) and the anodic domains by dark colors preceded by a sign (-).

III. Results and discussion

III.1. SVETmaps without corrosion inhibitors

The evolution of micro galvanic activity obtained under a wide range of anodic current is shown in Figure.2. Each map describes the micro galvanic activity of carbon steel electrode.

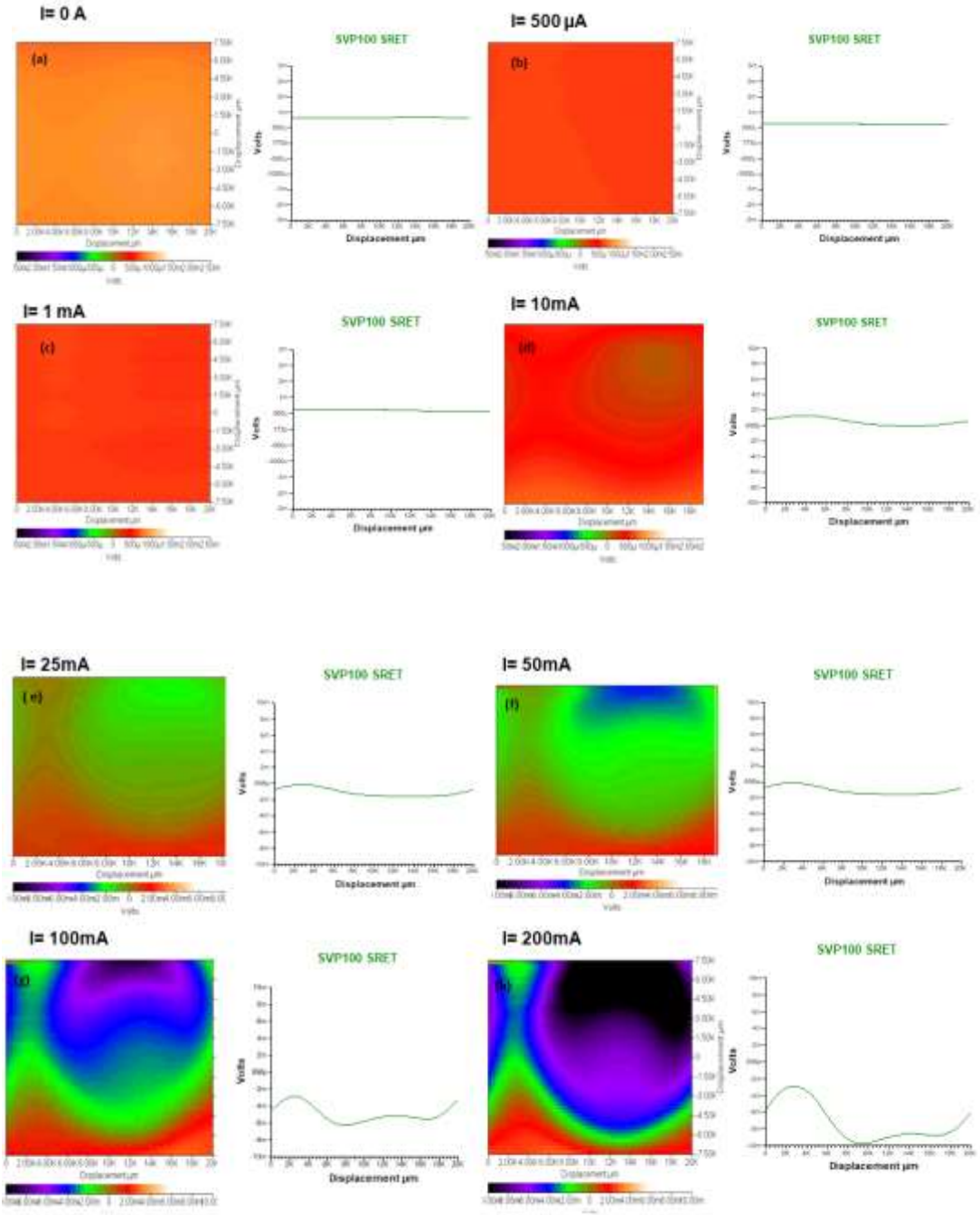

Figure 2. *Evolution of the microgalvanic activity of carbon steel API 5L X52, under imposed anodic currents of 0 A ,500µA, 1 mA 10mA, 25mA 50mA, 100mA and 200 mA.*

According to the cartographic obtained without corrosion inhibitors, the first anodic zone indicated by the green color appears on the center of the electrode at 10mA (Figure.2d); showing the heterogeneity in the behavior of the carbon steel. The microgalvanic potential is situated between -100µV and 700µV. Figure.2e illustrates the green color that predominates over the red color which appears at the end of the polarization at 25mA. This demonstrates the acceleration of the dissolution of the steel and the increase of microgalvanic activity obtained between -2 mV and 0 mV in the beginning of the polarization and 0 mV and +1mV at the end of the experiment.

At 50 mA (Figure.2f) the carthographic shows two anodic zones indicating the acceleration of the carbon steel dissolution and the increase of the microgalvanic activity. Blue coloration is observed in the beginning of the polarization followed by predominance of the green coloration. Cathodic zone represented by the red color is observed at the end of the experiment. This is confirmed by the microgalvanic potential which tends to anodic values situated between -5 mV in the beginning of

the test and +1 mV at the end. The dissolution of carbon steel is accelerated in the beginning of the experiment and slows down at the end. This is explained by the formation of protective layer on the swept surface of the electrode.
(Figure.2g) illustrate four anodic colors (black, purple, blue and green) in the center of the swept surface. The cathodic area characterized by the red color is observed in the extremity of the electrode. When 100mA is imposed, the most anodic zone appears in the beginning of the experiment where a very important microgalvanic activity is observed. The microgalvanic potential tends to a very anodic zone -9mV in the beginning of the experiment and +2 mV at the end.
At 200mA (Figure.2h) the carbon steel dissolution is widely increased. More anodic colors appear in the cartographic as: black, grey, purple, blue and green. The red color representing catholic zone appears at the end of the experiment. The electrochemical behavior shows that the most anodic zone appears in strength in the beginning of the experiment where a very important microgalvanic activity is observed (-10 mV to +2mV), leading to the apparition of less anodic areas. At the end of the test a very intensive dissolution of the steel is observed in the beginning of the experiment which tends to stabilize at the end, because of the covering of the surface electrodes by the products dissolution.
Several authors have investigated the localized corrosion as function of current on many metals. [33] have studied anti-corrosion performance of metal-rich coatings by integrating the overall anodic current density measured by scanning vibrating electrode technique (SVET). The total anodic current (and therefore the corrosion rate) over the coating surface was obtained and used to evaluate the galvanic interaction between coatings and substrates.

III.2. SVET maps in presence of corrosion inhibitors

Maps given in figures 3-10 were obtained under anodic polarization of wide range of currents and treated with two concentrations of inhibitors A and B (20 ppm and 50 ppm).
In the presence of the corrosion inhibitors A and B (Figure.3), the cartographics are similar to those obtained in absence of the inhibitors at 0A (Figure.2a). This means a negligible effect of the microgalvanic activity after the addition of corrosion inhibitors at a concentration of 50 ppm. No variation in the microgalvanic potential was registered which indicates the absence of the anodic zones.

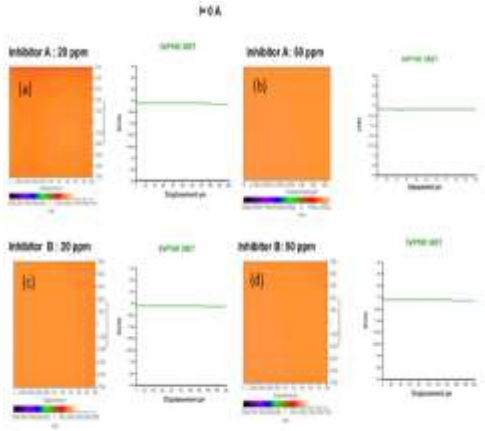

Figure 3 . *Effect of corrosion inhibitors A and B at 20 ppm and 50 ppm under I=0 A.*

At 500µA imposed current (Figure.4) the red color is dominant on all the swept surface in case of inhibitor A and a uniform orange color is observed with inhibitor B (Figure.4 c and d). Even in the presence of corrosion inhibitors, a less cathodic zone represented by the red color appears in the presence of inhibitor A at 20 ppm and 50ppm. The uniform orange color is observed in case of inhibitor B at both concentrations 20 ppm and 50 ppm which indicates the more effective cathodic protection of the steel due to the formation of a protective layer of inhibitor B which reduces the microgalvanic activity and the steel dissolution. This means that the adding of amine inhibitor with linear carbon chain (inhibitor A) is less efficient than amine inhibitor ramified with ethylene oxid (B) and it does not have effect on the electrochemical behavior of steel ; so no variation in the microgalvanic activity was observed.

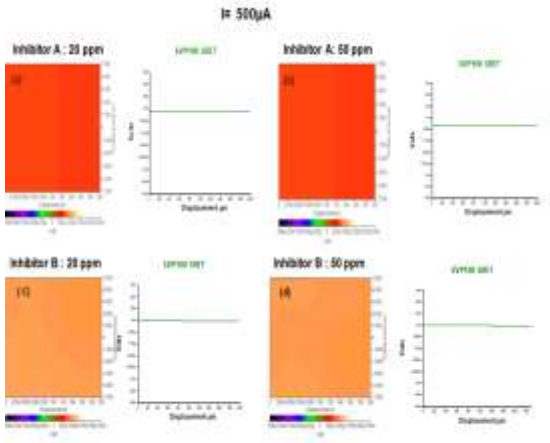

Figure 4. *Effect of corrosion inhibitors A and B at 20 ppm and 50 ppm under 500µA.*

Figure.5 shows the maps obtained at 1mA in the presence of both inhibitors at 20ppm and 50ppm. A uniform cathodic orange color is observed on the swept surface compared to maps obtained at the same current without inhibitors (Figure 2.c). These indicate the return to the cathodic zone due to the formation of a protective layer of inhibitors. The orange color is more intensive in case of the inhibitor A for the both concentrations. These indicate that inhibitor B is more efficient than inhibitor A which is less cathodic. Microgalvanic potential returns to its initial state (about 1000µV). The addition of corrosion inhibitors outweighs the imposition of current. A slight variation in microgalvanic activity is observed but it still remains in the cathodic domain.

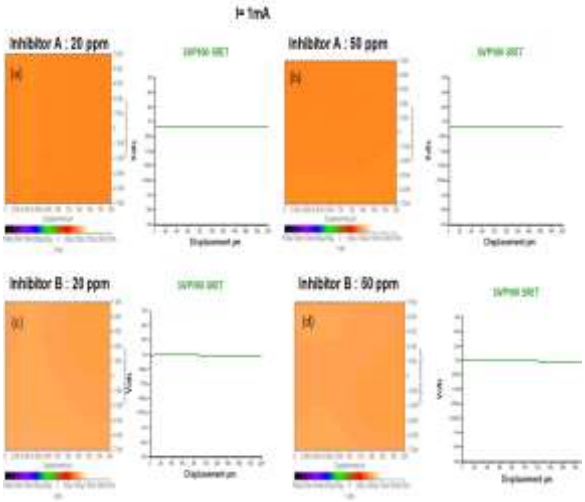

Figure 5. *Effect of corrosion inhibitors A and B at 20 ppm and 50 ppm under 1mA imposed current*

Figure.6 shows a significant change on the maps at 10 mA in the presence of the inhibitors compared to those obtained without the inhibitors at the same imposed current (Figure. 2 e). Only red and orange colors are observed in Figure.6 which indicate cathodic zone due to the presence of corrosion inhibitors. The less cathodic area characterized by the red color is more present in case of the inhibitor B (Figure.6 c and d). The anodic green color was very minimized for both inhibitors at 20ppm (Figure. 6 a and c) and its total disappearance is observed at 50 ppm (Figure 6 b and d) .The light microgalvanic activity is observed despite of the heterogeneity in the electrochemical behavior of the steel is observed. This affected the microgaolvanic potential situated between +200 µV and 1000 mV. The forming layer of inhibitor in both concentrations (20 ppm and 50ppm) has a weak effect on the microgalvanic activity of carbon steel.

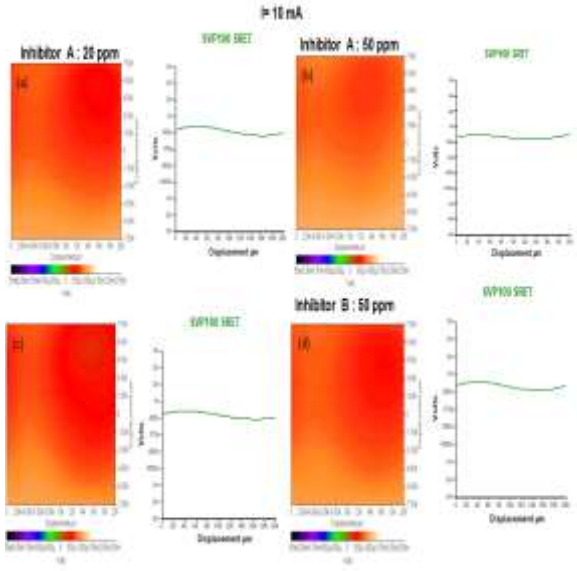

Figure 6. *Effect of corrosion inhibitors A and B at 20 ppm and 50 ppm under 10mA.*

In Figure.7, the efficiency of inhibitor A and B are not similar (Figure.7 a and c), (Figure.7 b and d) .Inhibitor A does not have any effect on the steel dissolution at 25 mA of imposed current. The green anodic color is persisting (Figure.7 a and b). The efficiency of inhibitor B at 50 ppm (Figure.7d) is more significant than inhibitor A at both inhibitors 'concentrations (Fig.7a and b). But with inhibitor B at 50 ppm the protection of the steel is more important but still insufficient for a good protection of the metal which is characterized by the diminution of the intensity of the anodic green color. . Microgalvanic potential is about -2mV to +1 mV for inhibitor A and -1mV to +1mV for inhibitor B.

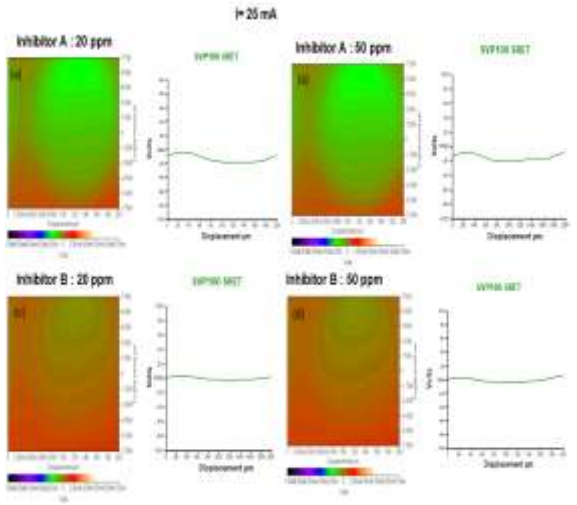

Figure 7. *Effect of corrosion inhibitors A and B at 20 ppm and 50 ppm under 25 mA.*

At 20 ppm (Figure. 8a), three areas were observed: blue and green for anodic zone and red color for the cathodic zone. In case of 50 ppm (Figure.8b); predominance of the green color is observed and a small area of red color indicating the catholic zone. Figure. 8c and d demonstrate only green and red colors for the both of concentrations (20 ppm and 50 ppm) in case of application of inhibitor B. This means that inhibitor B is more efficient than inhibitor A at 50 ppm. This efficiency is explained by the presence of ethylene in inhibitor B which increases the solubility of the inhibitor in aqueous medium contrary to aliphatic amine (inhibitor A) which shows less solubility in aqueous medium. The cartographic in Figure.8 shows the improvement of the protection from corrosion using corrosion inhibitors compared to maps obtained without inhibitors (Figure 2. f). The microgalvanic potential varied between -4mV and 1mV in presence of inhibitor A at 20 ppm and -2mV and +1 mV in case of utilization of inhibitor B and at 20 ppm and 50 ppm.

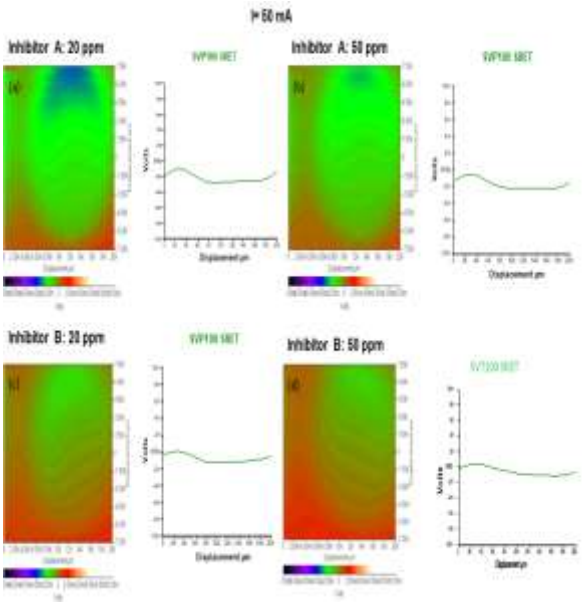

Figure 8. *Effect of the corrosion inhibitors A and B at 20 ppm and 50 ppm under 50 mA imposed current.*

Figure. 9 a and c show four anodic areas: purple, blue green and red for both inhibitors A and B at 20 ppm. At 50 ppm (Figure.9 b and d), disappearance of purple zone is observed. Only three anodic areas are present: blue, green and red color representing the cathodic zone. The cartographic shows that evolution of microgalvanic activity is less important compared to those given in the absence of the both corrosion inhibitors (Figure.2g); which explains the less anodic electrochemical behavior of the carbon steel. A slight variation of the microgalvanic potential is noticed. The potential varies respectively from -6mV to +2 mV in the presence of inhibitor A and B at 20 ppm and from – 4mV to +2 mV for the both inhibitors at 50 ppm. The addition of corrosion inhibitors is not effective at 20 ppm but at 50 ppm the dissolution of the steel is halted in the beginning of the experiment. This is due to the presence of the products dissolution and the corrosion inhibitor which tend to turn back the microgalvanic activity to the less anodic domains. In these experimental conditions, inhibitors A and B show similar anti-corrosive effect although inhibitor B is slightly more efficient than inhibitor A. This is due to the good adsorption of corrosion inhibitor by aliphatic amines which takes place by the following reaction [31]: $RNH_3^+(sol) <=> RNH_2+H^+ <=> RNH_2\text{-}Fe^0$

$RNH_2\text{-}Fe^0$ is an amine reagent that is chemically adsorbed. The chemical adsorption degree depends on the strength of amine-metal bands. Aliphatic amines are used as film-forming agents (inhibitor A). The efficiency of the protection in the presence of inhibitor A at 50 ppm may be related to the nitrogen atoms in the amino ($-NH_2$) functional group. Because of the high electron density, the nitrogen atom in aliphatic amines acts as a reaction center.

Furthermore, the long carbon chain in inhibitor A increases the adherence on the carbon steel surface. In the presence of the inhibitor B containing ethylene oxide, relatively higher corrosion inhibition was observed with 50ppm. This behavior can be due to the oxide function providing a high electron density for nitrogen which leads to the formation of acid base bond of Lewis between inhibitor and metal surface, this leads to greater protection and decrease of corrosion rate.

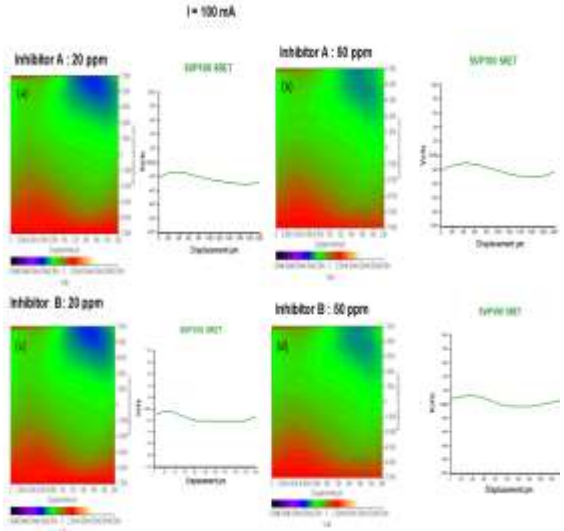

Figure 9. *Effect of the corrosion inhibitors A and B at 20 ppm and 50 ppm under 100 mA.*

In the presence of the both corrosion inhibitors at 200 mA (Figure.10), five anodic colors are observed in the carthocgraphic.Small black area, purple, blue, green and red, orange for the cathodic area. The black and purple areas showed in Figure.10 are smaller than those in (Figure.2h) which is due to the presence of corrosion inhibitors.
The increase of the inhibitors concentration from 20 ppm to 50ppm has an effect on the reduction of the intensive anodic area as black and purple colors (Figure.10 b and d). The inhibitor B at 50 ppm (Figure.10 d) shows a good performance to decrease the corrosion rate of the carbon that is demonstrated by the predominance of blue and green colors which are less anodic zone. It is insufficient for a good protection from corrosion.

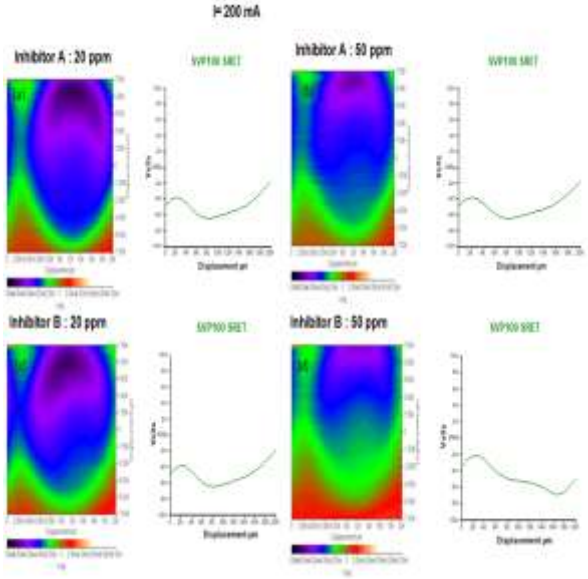

Figure 10. *Effect of the corrosion inhibitors A and B at 20 ppm and 50 ppm under 200mA.*

IV. Conclusion

The corrosion behavior of carbon steel API 5L X52 was studied in the absence and the presence of corrosion inhibitors based on primary amine with linear carbon chain (inhibitor A) and primary amine with branched ethylene oxide (inhibitor B) at imposed courant up to 200mA in aqueous medium by scanning vibrating electrode technique (SVET).
For the currents ranging from 0 A to 1000 µA, the carbon steel keeps a uniform activity during each experiment , but with a slight evolution following the change of colors of the maps given by SVET analysis which tends towards more anodic area. For currents in the order of mill amperes (mA); a strong evolution in the microgalvanic activity was observed considering the presence of several anodic areas, which causes the acceleration of the carbon steel dissolution characterized by the electronegative values of the microgalvanic potential. With corrosion inhibitors the apparition of the first anodic area was retarded to 25mA. Beyond this value, the protection becomes less important. The inhibitory power is better demonstrated in the presence of inhibitor B because of the good adsorption of ethylene oxide branched chain on the metal. The analysis of the microgalvanic activity allowed to:

1) Locate the fraction of the swept surface subjected to the corrosion through the cartographic.
2) Follow the adsorption of both the corrosion inhibitors at any point of the swept surface.

V. References

1. Wang, L .; Xin, J.; Cheng, L .; Zhao, K .; Sun, B .; Li, J. Influence inclusions on initiation of pitting corrosion and stress corrosion cracking of X70 steel in near-neutral pH environment. *Corrosion Science* 147 (2019) 108-127.
2. Heon-Young, H.; Tae-Ho, L.; Chang-Geun, L.; Hanme, Y. Comprehension of the relation between pitting corrosion resistance and phase fraction of S32101 duplex stainless steel. *Corrosion Science* 149 (2019) 226-235.
3. Chen, A.; Chen, F.; Cao, X.; Liao, W.; Liu, L.; Zheng, J.; Zhang, C.; Cao, C. Study of pitting corrosion on mild steel inwet–dry cycles by electrochemical noise analysis based on chaos theory. *Corrosion Science* 66 (2013) 183–195.
4. Isaacs, H.S.; Huang, S.; Jovancicevic, V. Location of corrosion on iron and carbon steel surfaces with crevices. *Journal of Electrochemical. Society* 143 (1996) 178–180.
5. Li, Y .; Xu, N.; Guo, X.P.; Zhang, G. The role of acetic acid or H + in initiating crevice corrosion of N80 carbon steel in CO 2 -saturated NaCl solution. *Corrosion Science* 128 (2017) 9-22.
6. Aoyama, T.; Sugawara, Y.; Muto, I.; Hara, N. In situ monitoring of crevice corrosion morphology of Type 316L stainless steel and re-passivation behavior induced by sulfate ions. *Corrosion Science* 127 (2017) 131–140.
7. Oliveira, S.; Limaa, M.; Franca¸F.; Vieira, M.; Silva,P.; Urtiga Filho, S. Control of microbiological corrosion on carbon steel with sodium hypochlorite and biopolymer. *International journal of microbiological molecules* 88 (2016) 27-35.
8. Wu, T.; Yan, M.; Xu, J.; Liu, Y.; Sun, C.; Ke, W. Mechano-chemical effect of pipeline steel in microbiological corrosion. *Corrosion Science* 108 (2016) 160-168.
9. Erika, M.; Suarez, K.; Lepkova, B.; Kinsella,L.; Machuca,L. Aggressive corrosion of steel by a thermophilic microbial consortium in the presence and absence of sand. *International Biodeterioration & Biodegradation* 137 (2019) 137–146.
10. Isaacs, HS. The measurement of the galvanic corrosion of soldered copper using the scanning vibrating electrode technique. *Corrosion Science* 28 (1988) 547– 558.
11. Soltis, J.; Lichti, KA. Galvanic corrosion of carbon steel coupled to antimony. *Corrosion Science* 68 (2013) 162-167.
12. Keith, A.; Lichti, M.; Lily, W. Galvanic corrosion study of carbon steel to arsenic and antimony couples. *Geothermics* 58 (2015) 15-21.
13. Zhiming, S.; Jimmy, X.; Andrej, A. Galvanostatic anodic polarisation of WE43. *Journal of Magnesium and Alloys* 2 (2014) 197-202.

14. Gopi, D.; Govindaraju, K.M.; Collins,V.; Prakash, A.; Sakila, A.; Kavitha,L. A study on new benzotriazole derivatives as inhibitors on copper corrosion in ground water. *Corrosion Science* 51 (2009) 2259-2265.
15. Pust, S.E.; Maier, M.; Wittstock, G. Investigation of localized catalytic and electrocatalytic processes and corrosion reactions with scanning electrochemical microscopy (SECM). *Zeitschrift für Physikalische Chemie* 222 (2008) 1463–1517.
16. Niu, L.; Yin, Y.; Guo, W.; Lu, M.; Qin, R.; Chen, S. Application of scanning electrochemical microscope in the study of corrosion of metals. *Journal of Materials Science* 44 (2009) 4511–4521.
17. Souto, R.M.; Lamaka, S.V.; González, S. Uses of scanning electrochemical microscopy in corrosion research. *Science, Technology, Applications and Education*. 3(2010) 1769–1780.
18. Tada, E.; Sugawara, K.; Kaneko, H. Distribution of pH during galvanic corrosion of Zn/steel surface. *Electrochimca Acta* 49 (2004) 1019–1026.
19. Coelhoa, L.B.; Oliviera,B. The inhibition efficiency of different species on AA2024/graphite galvanic coupling models depicted by SVET. *Corrosion Science* 136 (2018) 292–303
20. Souto,RM.; Gonzalez-Garcıa,Y.; Bastos, A.C.; Simoes, A.M. Investigating corrosion processes in the micrometric range: A SVET study of the galvanic corrosion of zinc coupled with iron. *Corrosion Science* 49 (2007) 4568–4580.
21. Fateh, A.; Aliofkhazraei, M.; Rezvanian, A.R. Review of corrosive environments for copper and its corrosion inhibitors. *Arabian Journal of Chemistry* 13 (2020) 481–544.
22. Hamadi,L.; Mansouri, S.; Oulmi, K.; Kareche, A.The use of amino acids as corrosion inhibitors for metals: a review. *Egyptian journal of petrolium* 27 (2018) 1157-1165.
23. Samiento, E.; Bustos, J.G.; González-Rodriguez, J.; Uruchurtu, G.; Dominguez-Patiño, M.; Salinas, B. Effect of inorganic inhibitors on the corrosion behavior of 1018 carbon steel in the LiBr + ethylene glycol + H2O mixture. *Corrosion Science* 20(2008) 2296-2303.
24. Muster, T.H.; Hughes, A.E.; Furman, S.A.; Harvey, T.; Sherman, N.; Hardin, S.; Corrigan,P.; Lau, D.; Scholes, F.H.; White, P.A.; Glenn, M.; Mardel, J.; Garcia, S.J. A rapid screening multi-electrode method for the evaluation of corrosion inhibitors. *Electrochimica Acta* 54 (2009) 3402-3411.
25. Aldana-Gonzalez, J.;Espinoza-Vazquez, A.; Romero-Romo, M.; Uruchurtu-Chavarin, J.; Palomar-Pardave, M. Electrochemical evaluation of cephalothin as corrosion inhibitor for API 5L X52 steel immersed in an acid medium. *Arabian Journal of Chemistry* 12 (2019) 3244-3253.
26. Abdallah, Y. M.; Shalabi, K.; Bayoumy, N. M. Eco-friendly synthesis, biological activity and evaluation of some new pyridopyrimidinone derivatives as corrosion inhibitors for API 5L X52 carbon steel in 5% sulfamic acid medium. *Journal of Molecular Structure* 1171 (2018) 658–671.
27. Garcia-Arriaga, V.; Alvarez-Ramirez, J.; Amaya, M.; Sosa, E. H_2S and O_2 influence on the corrosion of carbon steel immersed in a solution containing 3 M diethanolamine. *Corrosion Science* 52 (2010) 2268-2279.
28. Martinez, D.; Gonzalez, R.; Montemayor, K.; Juarez-Hernandez, A.; Fajardo, G.; Hernandez-Rodriguez, M. A. L. Amine type inhibitor effect on corrosion–erosion wear in oil gas pipes. *Wear* 267 (2009), 255–258.
29. Choi, H.; Young Kim, K.; Myung, J. Encapsulation of aliphatic amines into nanoparticles for self-healing corrosion protection of steel sheets. *Progress in Organic Coatings* 76 (2013) 1316–1324.
30. Ogle, K.; Morel, O.; Jacquet, D. Observation of self-healing functions on the cut edge of galvanized steel using SVET and pH microscopy. *Journal of the Electrochemical Society* 153 (2006) 1–5.
31. Bastos, A.C.; Ferreira, M.G.; Simoes, A.M. Corrosion inhibition by chromate and phosphate extracts for iron substrates studied by EIS and SVET. *Corrosion Science* 48 (2006) 1500–1512.
32. Askari, M.; Aliofkhazraei, M.; Ghaffari, S.; Hajizadeh, A. Film former corrosion inhibitors for oil and gas pipelines - A technical review. *Journal of Natural Gas Science and Engineering* 58 (2018) 92-114.
33. Yan, M.; Gelling, V.J.; Hinderliter, B.R.; Battocchi, D.; Tallman, D.E.; Bierwagen, J.P. SVET method of anti-corrosion performance characterization of metal-rich coatings. *Corrosion Science* 52 (2010) 2636–2642.

Please cite this Article as:
Ouarzki I., Bounoughaz M., Investigation of microgalvanic activity of carbon steel API 5L X52 in presence of Amine corrosion inhibitors by scanning vibrating electrode technique (SVET), ***Algerian J. Env. Sc. Technology***, **9:1 (2023) 2997-3005**